

X-RAY CT HIGH DENSITY ARTIFACT SUPPRESSION IN CRYOSURGERY

Laigao Chen¹, Yun Liang², Lisa X. Xu³, Jikun Wei¹, George A. Sandison¹¹School of Health Sciences, Purdue University, West Lafayette, IN 47907²Department of Radiology, Indiana University Medical School, Indianapolis, IN 46202³School of Mechanical Engineering, Purdue University, West Lafayette, IN 47907**Abstract:**

X-ray CT provides imaging guidance for cryosurgery that allows 3D visualization of frozen and unfrozen tissue. Temperature in the tissue water-ice interface (0 to -10°C) may be calibrated to Hounsfield units. However x-ray CT images and their thermal calibration can be compromised by the cryoprobes generating high-density streak artifacts. A new subtraction technique for suppression of these artifacts is proposed and tested in prostate cryosurgery simulations. By subtracting the profile without cryoprobes from the profile with cryoprobes and iceballs, we can get the combined profile of the cryoprobes and a low value background. A polynomial interpolation is performed to obtain the background profile, which is then added back to the original profile without probes. The resulting profile is then fed to a conventional filtered back-projection routine to reconstruct the probe-free image. Finally the cryoprobe pixels in the originally constructed image with probes are added back to the probe-free image to get the final artifact-suppressed image. The major advantage of this subtraction technique is that it can successfully suppress the high-density artifacts in bone abundant body regions. X-ray CT images of cryoprobe arrays in a homogeneous gelatin phantom and the pelvic region of an anthropomorphic Rando phantom containing a human skeleton were generated. After suppression, cryoprobe metal artifact streaks are reduced and visualization of the positions and dimensions of the cryoprobes are well preserved. In-vivo canine studies are planned to test this new suppression technique for cryosurgery use.

Introduction:

Cryosurgery is a therapeutic procedure to ablate tissue by freezing injury. Hollow metallic tubes, known as cryoprobes, within which a gas or liquid cryogen is caused to flow are implanted in the tissue and ablating iceballs grow about them. Image guidance in cryosurgery

is usually performed using ultrasound. However x-ray CT imaging is an alternative means of guidance having the advantage of displaying 3D structure of the iceball, including any tissue architecture within. Another advantage of the x-ray CT modality is that temperature in the density change region of the water-ice interface can be calibrated to allow almost real-time isotherm contour overlays on the iceball images. Unfortunately, the x-ray CT images are compromised by the presence of artifacts caused by the array of metal cryoprobes [1-6]. One major source of metal artifacts in CT images is the beam hardening correction typically used in commercial CT scanners. CT reconstruction theory assumes that the incident x-ray beam is mono-energetic. In practice the x-ray beam in commercial CT scanners is poly-energetic and typically contains an energy spectrum from 20keV to 120keV or 140keV. To remedy this problem, CT manufacturers typically apply a polynomial correction function to the measured attenuation data to approximate the ideal attenuation data for a mono-energetic x-ray beam [7]. This beam hardening correction function is usually derived and calibrated for body tissues and is therefore not accurate for metal objects. Broad dark streaks emanating from the cryoprobes result in the reconstructed CT image. Another important source of these metal streak artifacts stems from the poor signal-to-noise ratio due to photon starvation of the projection rays passing through the high attenuation metal cryoprobes. Resulting high fluctuations in the photon number for these projection rays lead to thin streaks (alternately dark and bright) along radial directions in the reconstructed image.

In this paper, we propose a subtraction technique to reduce the artifacts caused by cryoprobes. This technique significantly suppresses the artifacts while still faithfully reproducing the positions and dimensions of the cryoprobes. Furthermore, the suppression technique is computationally efficient and easily adapted to commercial CT systems.

Methods:

The region of interest is scanned before the cryoprobes are inserted and scanned again after the cryoprobes are put in place. (Repeated scanning is required to follow the evolution in growth of the iceball formed during a typical freezing procedure). Hereafter we will use $P_1(m,n)$ to denote the parallel beam projection profile from the first scan, namely the one without any cryoprobe; and similarly $P_2(m,n)$ for profile from the second scan. And $m=1,2,\dots,M$, $n=1,2,\dots,N$ are the indices of detectors and projection views respectively. If the original scanning geometry is in fan beam format, we assume it has already been rebinned to parallel beam format. These two profiles then go through the following steps to reduce the artifacts.

Step 1: Finding the metal probe regions in the profile. A conventional filtered back-projection routine is applied to reconstruct an initial image from $P_2(m,n)$. Metal probe pixels are extracted with a suitable threshold, which is normally 2000~3000 HU, from the initial image. For each view, the metal pixels are reprojected to form clear delineation of their corresponding projection channels. Instead of the typical projection ray driven reprojection technique [8], pixel driven reprojection technique is used. Specifically, each metal pixel is reprojected onto all view angles. This pixel driven reprojection technique is very computational efficient in our particular application due to the fact that the total number of metal pixels only occupy a very small portion of the whole image matrix. Then the metal probe regions in the profile can be determined as:

$$R(n) = \{[s(i,n), e(i,n)]\}, \quad i=1,\dots,I(n) \quad (1)$$

where $I(n)$ is the total number of metal probe regions within the n -th projection view; $s(i,n)$ and $e(i,n)$ are the starting and ending channels of the i -th metal probe region within the n -th projection view.

Step 2: Subtraction and interpolation. By subtracting $P_1(m,n)$ from $P_2(m,n)$, which is the profile with the presence of cryoprobes and iceballs, we get the combined profile of the probes and a background.

$$P_3(m,n) = P_2(m,n) - P_1(m,n) \quad (2)$$

There are several reasons for the presence of the low value background profile: (a) Since the density of ice is slightly lower than that of body tissues, there will be a negative background profile; (b) Body tissues may move a little during cryosurgery; (c) Intrinsic randomness of x-ray absorption and detection differences between two scans.

A baseline profile $B(m,n)$ can be obtained for all regions in $R(n)$ by performing a polynomial interpolation to the projection data on both sides of the metal probe region $[s(i,n), e(i,n)]$. We denote this interpolation as an operator \hat{O} :

$$B(m,n) = \hat{O} P_3(m,n) \quad (3)$$

Then this background profile is added back to the profile without probes $P_1(m,n)$ to get the probe-free profile.

$$P(m,n) = P_1(m,n) + B(m,n) \quad (4)$$

Step 3: Filtered back-projection and adding back of the probe pixels. $P(m,n)$ in Eq.(4) is the processed final profile that is fed to a conventional filtered back-projection routine to reconstruct the artifact-suppressed image. Those metal probe pixels obtained from step 1 by thresholding are now added back to the reconstructed image so as to reproduce the probes in the same positions and with the same dimensions.

Overall, the above processing procedure in the projection profile domain can be expressed as:

$$P(m,n) = P_1(m,n) + \hat{O} [P_2(m,n) - P_1(m,n)] \quad (5)$$
 and it can be automated and easily implemented on current commercial CT scanners.

To illustrate the above procedure, the new method has been applied to a homogeneous gelatin phantom. As proposed, an axial CT scan was performed without any probe or iceball. Then five cryoprobes were inserted into the phantom to form a pentagon shape. An argon cryogen was used with the probes to cause the gelatin to freeze and form an iceball around each probe. After all five iceballs coalesced to be a single one, a second scan was performed. The whole phantom volume scanned comprised 32 images of slice thickness 2.5mm.

To also test this subtraction method in the presence of bone structures, the pelvic region of an anthropomorphic Rando phantom (Phantom Laboratory Inc., Salem, NY) was used. The anthropomorphic Rando phantom represents an average man made from tissue-equivalent materials that is transected into transverse slices of 2.5 cm (1 in.) thickness. When assembled the 36 slices, numbered 0-35, provide a head and torso with skeleton, lungs, and air passages. Scans of the phantom and five cryoprobes were obtained for slices 33 and 34.

All CT scans were performed on a Philips MX8000 quad-slice spiral CT scanner (Philips Medical Systems). The scanning

parameters set were 120 kVp, 250 mA and slice thickness 2.5 mm. After scanning, the raw projection data were downloaded from the scanner to a SUN workstation. All the following processing procedures including rebinning, filtered back-projection and metal artifacts suppression were implemented on the SUN workstation using Interactive Data Language (Research Systems, Inc.). For the 3D rendering of the homogeneous gelatin phantom, the reconstructed image sets before and after correction are sent back to a dedicated view workstation of the MX8000 CT scanner (Philips Medical Systems) for, multi-planar reformation (MPR) and maximum intensity projection (MIP).

Results and Discussions:

As shown in Fig. 1(a), for the homogenous gelatin phantom, severe streak artifacts in the original x-ray CT image were caused by the cryoprobes. After correction, the major high density streak artifacts are successfully reduced, as shown in Fig. 1(b). The correction is not perfect and a few new artifacts are introduced due to the intrinsic inconsistency of the polynomial interpolation among different projection profiles. Fig. 1(c) and Fig. 1(d) are 3D renderings of the cryoprobes and iceballs. Before correction, the iceballs are rendered in irregular shapes because of the streak artifacts while after correction the five iceballs are clearly rendered around each cryoprobe. Fig. 2(a,b,c) illustrate one of the projection profiles and its correction procedure. In Fig. 2(a) the solid line is the original profile where the peaks are due to the pentagon shaped array of metal cryoprobes. The dotted line is the profile before the probes were inserted to the phantom. Because the density of ice is lower than that of gelatin, the dotted line is a little higher than the solid line. After subtraction, we get the solid curve in Fig. 2(b) and perform the interpolation which is plotted as dotted line in this figure. Then the dotted line profile in Fig. 2(b) is added back to the dotted line profile in Fig. 2(a) and the result is plotted in Fig. 2(c), where the dotted line profile in this figure is the final processed profile that is fed to a back-projection routine to reconstruct the probe-free image.

For the pelvic region of the Rando phantom which has large bone structures, Fig. 3(a) shows the original reconstructed image with streak artifacts emanating from the probes. Fig. 3(b) is the result after applying this new subtraction technique. Since it is not possible to form iceballs in the Rando phantom because it is

resin-based, the background profile mainly comes from the random noise of the two scans. Therefore a zero interpolation baseline was used. It is clearly shown that metal probe artifacts are successfully removed.

This artifact suppression technique does not require body tissues be fixed between the two x-ray scans because an interpolation is used to simulate the tissue profile. However, the bone structures do need to be well fixed between scans since the bone structure profile is difficult to simulate by interpolation. Movement of bony structure may be minimized by, for example, a stereotactic body frame [9]. Such frames may have an added bonus that is precision guidance of the cryoprobes.

References:

- [1] Glover GH, Pelc NJ. "An algorithm for the reduction of metal clip artifacts in CT reconstructions." *Med. Phys.* **8**: 799-807, 1981.
- [2] Kalender WA, Hebel R, Ebersberger J. "Reduction of CT Artifacts Caused by Metallic Implants." *Radiology* **164**: 576-577, 1987.
- [3] Zhao S, Robertson DD, Wang G, Whiting B, Bae KT. "X-ray CT metal artifact reduction using wavelets: an application for imaging total hip prostheses." *IEEE Trans. Med. Imaging* **19**: 1238-1247, 2000.
- [4] Wang G, Snyder DL, OSullivan JA, Vannier MW. "Iterative deblurring for CT metal artifact reduction." *IEEE Transactions on Medical Imaging*, **15**: 657-664, 1996.
- [5] Tuy H K. "A post-processing algorithm to reduce metallic clip artifacts in CT images." *European Radiology* **3**: 129-134, 1993.
- [6] De Man B, Nuyts J, Dupont P, Marchal G, Suetens P. "An iterative maximum-likelihood polychromatic algorithm for CT." *IEEE Trans. Med. Imaging* **20**: 999-1008, 2001.
- [7] Herman GT. "Correction for beam hardening in computed tomography." *Phys. Med. Biol.* **24**: 81-106, 1979.
- [8] Crawford CR. "Reprojection using a parallel back-projector." *Med.Phys.* **13**: 480-483, 1986.
- [9] Lax I, Blomgren H, Naslund I and Svanstrom R. "Stereotactic radiotherapy of malignancies in the abdomen." *Acta Oncologica*, **33**: 677-683, 1994.

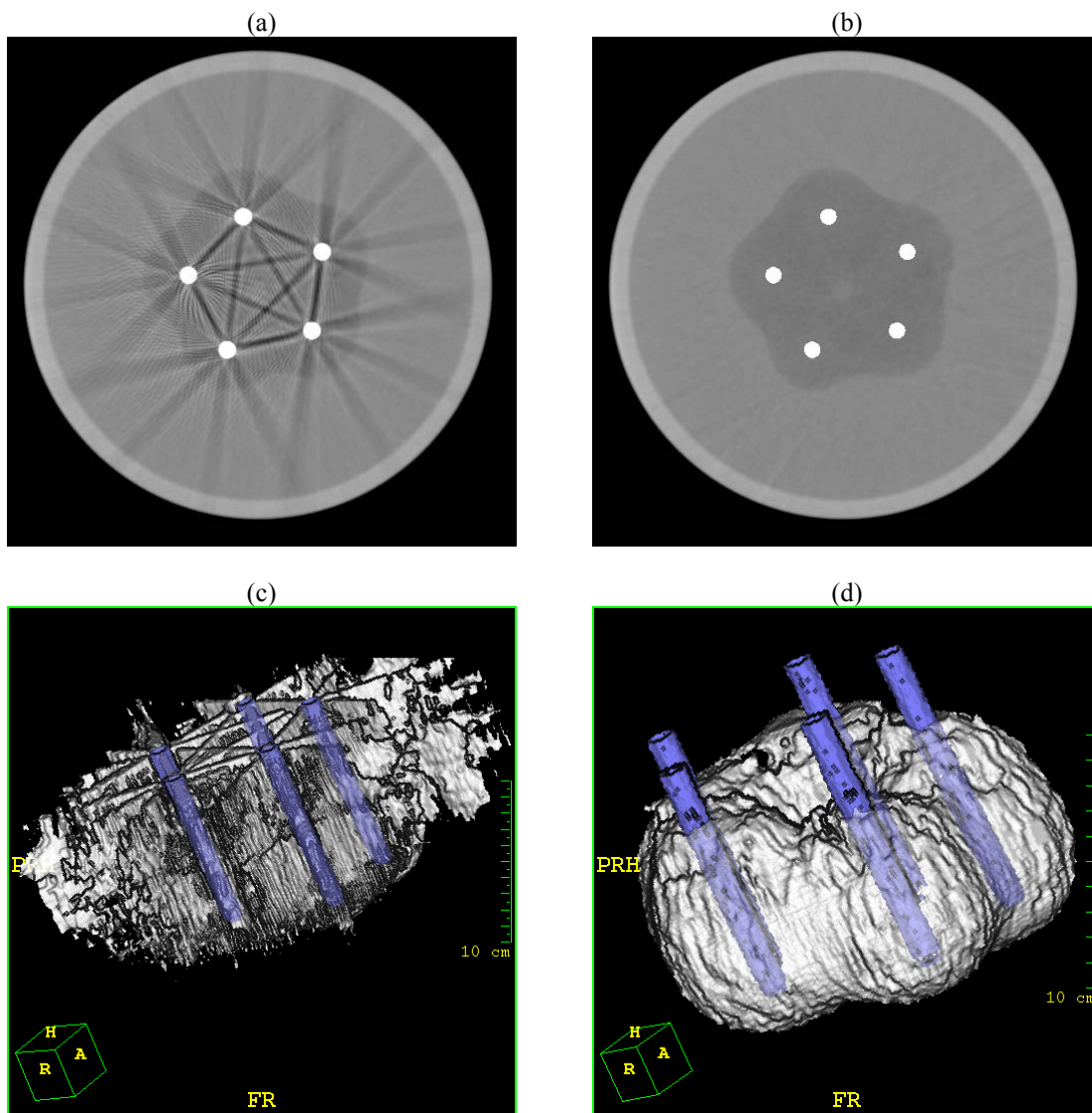


Figure 1. Comparison of CT images of cryoprobes and iceballs in a homogeneous gelatin phantom before and after correction. (a) image before correction; (b) image after correction. (c) 3D rendering before correction; (d) 3D rendering after correction.

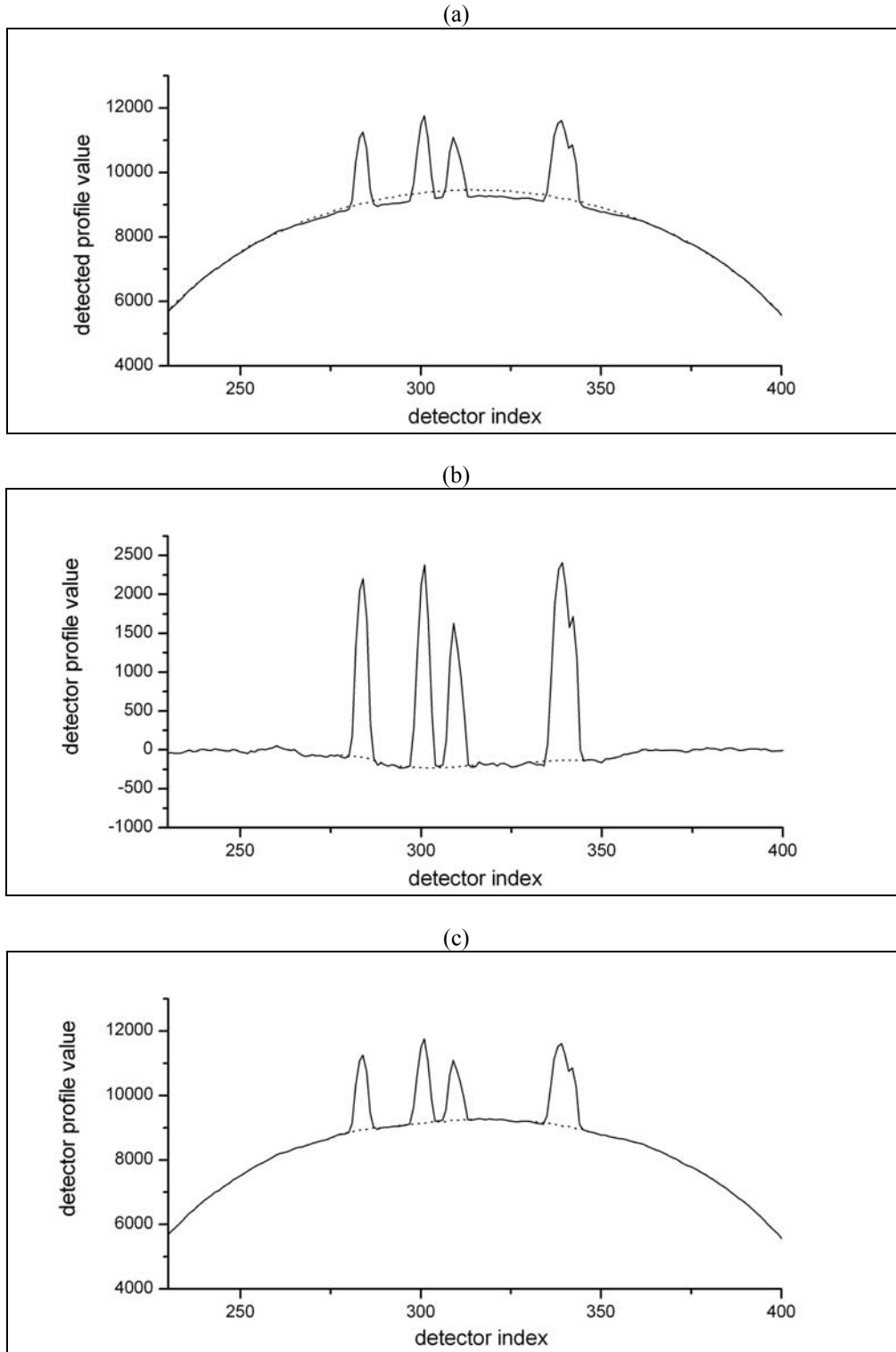


Figure 2. Diagrams of the subtraction technique procedure. (a) The two original projection profiles, solid line is the one with probes and iceballs, dotted line is without any probe or iceball. (b) Combined profile of the cryoprobes and the background, obtained by subtracting dotted line from solid line in (a). Then interpolation is performed and represented by the dotted line. (c) Resultant profile after adding the interpolated background back.

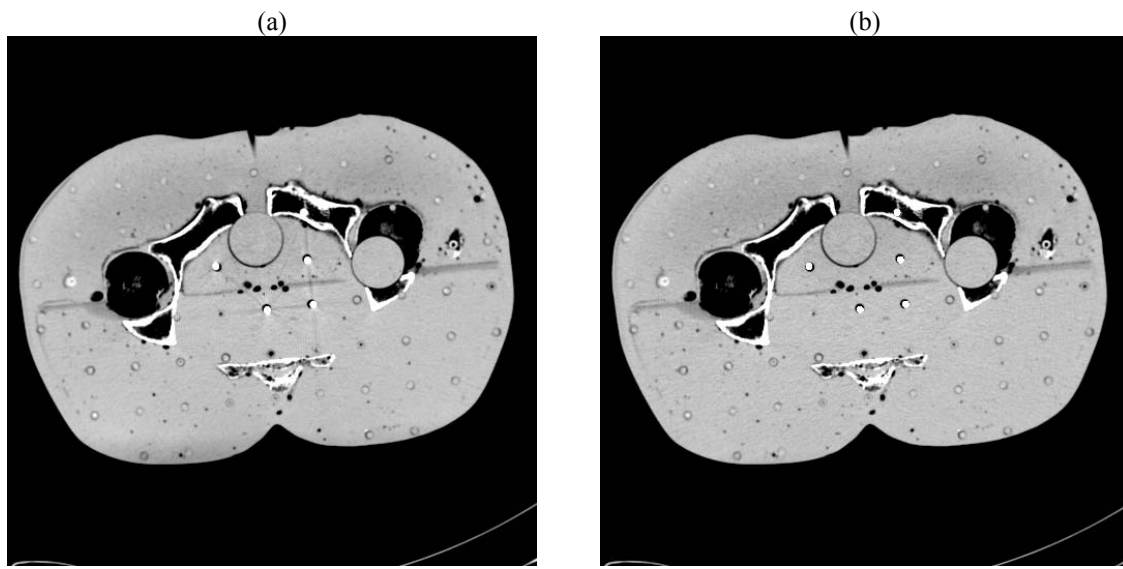


Figure 3. CT images of the pelvic region of an anthropomorphic Rando phantom. (a) image before correction, there are streak artifacts emanating from the cryoprobes; (b) image after subtraction method, metal probe artifacts are removed without introducing bone artifacts. The dark areas surrounding the bright circular cryoprobes are due to air inside the holes made for holding the cryoprobes.